Available online at www.sciencedirect.com
ScienceDirect
Ceramics International 35 (2009) 943–947
CERAMICS INTERNATIONAL
www.elsevier.com/locate/ceramint

Magnetic and thermal expansion properties of chromium-substituted lithium ferrite

Yen-Pei Fu [a,*], Shaw-Bing Wen [b], Chun-Cheng Yen [a]

[a] Department of Materials Science and Engineering, National Dong-Hwa University, Shou-Feng, Hualien 974, Taiwan
[b] Meiho Institute of Technology, Neipu, Pingtung 912, Taiwan

Received 21 January 2008; received in revised form 4 February 2008; accepted 12 March 2008
Available online 2 July 2008

Abstract

The structure, magnetic, and thermal expansion properties of chromium-substituted lithium ferrite have been investigated. The lattice constant (Å) decreases linearly as $a\ (x) = 8.32366 - 0.04338x$ for $Li_{0.5}Fe_{2.5-x}Cr_xO_4$ ($x = 0.0$–1.0). When increasing Cr content, the initial permeability decreased gradually. The average thermal expansion coefficient of $Li_{0.5}Fe_{2.5-x}Cr_xO_4$ ($x = 0.0$–1.0) varied from 15.34 to 17.77 ppm/°C, with increasing Cr content, the average thermal expansion coefficient decreased. The average thermal expansion coefficient (ppm/°C) in the range of 25–850 °C give the polynomial correlation as follows, TEC $(x) = 1\ 7.775 - 0.216x - 0.723x^2 - 1.493x^3$ for $Li_{0.5}Fe_{2.5-x}Cr_xO_4$ ($x = 0.0$–1.0).

Keywords: A. Powders: solid state reaction; C. Thermal expansion; C. Magnetic properties; D. Ferrite; E. Soft magnets

1. Introduction

Lithium and substituted lithium ferrites have attracted the attention of scientists for a long time and have been developed as a replacement for yttrium iron garnet (YIG) owing to their low cost [1]. Lithium ferrites are important components of microwave devices and memory cores owing to their high Curie temperature, high saturation magnetization, and hysteresis loop properties, which offer performance advantage over other spinel structures [2–5]. Since the number of ferric ions on A and B sites is unequal in lithium ferrite, the calculated magnetic moment is not just that of lithium ions, but is given by the difference in the magnetic moment of ions on A and B sites. Consequently, lithium ferrite possesses a higher Curie temperature than other spinel ferrites [6]. On the other hand, lithium ferrites have been also promising substitutes for Ni–Cu–Zn ferrites in advanced planar ferrite devices, because of their low sintering temperature, high Curie temperature and excellent electromagnetic properties at high frequency [7].

In this paper, we describe the results of magnetic and thermal expansion properties for Cr-substituted lithium ferrite. The effect of Cr content on lattice parameter, initial permeability, and thermal expansion properties for the sintered $Li_{0.5}Fe_{2.5-x}Cr_xO_4$ specimens were investigated.

2. Experimental procedure

Chromium-substituted lithium ferrite $Li_{0.5}Fe_{2.5-x}Cr_xO_4$ with $0.0 < x < 1.0$ were prepared following the ceramic method. Samples were prepared from reagent-grade powders of Li_2CO_3, Cr_2O_3, and Fe_2O_3. Mixtures were ball-milled for 12 h in distilled water, dried, and calcined at 700 °C for 4 h. Subsequently the powder was remilled, granulated, and pressed into pellets under a uniaxial pressure of 1000 kg f/cm^2. Pellets were sintered at 1200 °C for 4 h in air.

A computerized X-ray powder diffractometer (XRD, Rigaku D/Max-II) with Cu Kα radiation with $\lambda = 0.154178$ nm was used to identify the crystalline phase and calculate lattice parameter, theoretical density, and cell volume. A vibrating sample magnetometer (VSM) was used to measure the saturation magnetization (M_s) and intrinsic coercive force (H_c) of the calcined $Li_{0.5}Fe_{2.5-x}Cr_xO_4$ powders at room temperature. The initial permeability (μ_i) of Cr-substituted lithium ferrite were measured on an Hewlett-Packard 4194A impedance analyzer in the frequency range of 1 kHz to 100 MHz; 15 turns of coil were wound around the sintered

* Corresponding author. Tel.: +886 3 863 4209; fax: +886 3 863 4200.
E-mail address: d887503@alumni.nthu.edu.tw (Y.-P. Fu).

0272-8842/$34.00
doi:10.1016/j.ceramint.2008.03.013

toroidal specimens. The thermal expansion coefficients of sintered $Ce_{0.8}Sm_{0.2}O_{1.90}$ pellets were measured by dilatometer (DIL; Netzsch DIL 402 PC) using a constant heating rate of 10 °C/min in the temperature range of 25–850 °C.

3. Results and discussion

Fig. 1 illustrates the X-ray diffraction patterns of the $Li_{0.5}Fe_{2.5-x}Cr_xO_4$ specimens sintered at 1200 °C for 4 h. It is evident that the $Li_{0.5}Fe_{2.5-x}Cr_xO_4$ specimens contain the lithium ferrite phase. All the peaks in the pattern are matched well with JCPDS card (no. 38-0259). No secondary phases are detected in the XRD patterns of samples. The introduction of Cr^{3+} ions into $Li_{0.5}Fe_{2.5}O_4$ can cause a small shift to higher diffraction angle in the lithium ferrite peaks. This shift is indicative of the change in lattice parameter. Moreover, doping Cr^{3+} ions also decrease the diffraction intensity in X-ray diffraction pattern for $Li_{0.5}Fe_{2.5-x}Cr_xO_4$ powder. It reveals evidently that $Li_{0.5}Fe_{2.5}O_4$ possesses higher intensity than the rest of the samples. The calculation of the lattice parameters was carried out using the one main reflection typical of a spinel structure material with a cubic cell, corresponding to the (3 1 1), (2 2 0), and (5 1 1) planes. The lattice parameter was calculated according to the formula $\sin^2\theta/(h^2+k^2+l^2) = \lambda^2/4a^2$, where λ is Cu Kα radiation with 1.5405 Å, θ is diffraction angle.

Several authors have discussed the lattice parameter of $Li_{0.5}Fe_{2.5-x}Cr_xO_4$ [8–11]. Kuznetsov et al. reported self-propagating high-temperature synthesis of $Li_{0.5}Fe_{2.5-x}Cr_xO_4$ ($0 \leqq x \leqq 2.0$) and Fernandez-Barquin et al. reported Rietveld analysis and magnetic properties of $Li_{0.5}Fe_{2.5-x}Cr_xO_4$ ($0 \leqq x \leqq 2.0$). Gorter reported that the lattice parameter of $Li_{0.5}Fe_{2.5-x}Cr_xO_4$ decreases linearly with increasing amount of $x < 0.5$. However, in the range of $0.5 < x < 1.25$, decreasing rate of the lattice parameter gradually reduces as x increases [11]. In the present study, we also observed this phenomenon. Fig. 2 shows the dependence of lattice constant versus Cr content. The lattice constant decreased markedly with increasing amount of chromium in the range of $0.0 \leqq x \leqq 0.5$, and in the range of $0.5 \leqq x \leqq 1.0$, the lattice parameter gradually decrease as x increases. As the Cr concentration increases, the lattice constant (Å) decreases linearly as $a\ (x) = 8.32366 - 0.04338x$ for $Li_{0.5}Fe_{2.5-x}Cr_xO_4$ ($x = 0$–1.0). This indicates different of Fe^{3+} (0.64 Å) and Cr^{3+} (0.62 Å) in an oxide solid solution with a spinel-type structure. When doped with smaller sized Cr^{3+} ions, the spinel lithium ferrite will shrink. Doping Cr^{3+} ions in a spinel-type structure will induce uniform strain in the lattice as the material is elastically deformed. This effect causes the lattice plane spacing to change and the diffraction peaks shift to a higher 2θ position. It is noticeably that the lattice parameter is nonlinear of Cr content for $Li_{0.5}Fe_{2.5-x}Cr_xO_4$. According to Gorter's report, he defined chemical formula of $(Fe_{1.0})[Li_{0.5}Fe_{1.5-x}Cr_x]O_4$ and $(Fe_{1.0-y}Li_y)[Li_{0.5-y}Fe_{1.5-x+y}Cr_x]$ for $x = 0$ and $x > 0$, respectively. The formula for $x > 0$ indicates that Li^+ ions partially occupy tetrahedral (A) site and distribution of Fe^{3+} ions on tetrahedral (A) site and octahedral [B] site change. y increases nonlinearly as x increases [9]. The observed nonlinear Cr content dependence of lattice parameter may be resulting from the change of ion distribution depends on the amount of Cr substitution. The theoretical density was calculated according to the formula $D_x = 8M/Na^3$, where M is the molecular mass, N is Avogadro's numder, and a is the lattice parameter which was calculated from the X-ray diffraction pattern. The theoretical density is in the range of

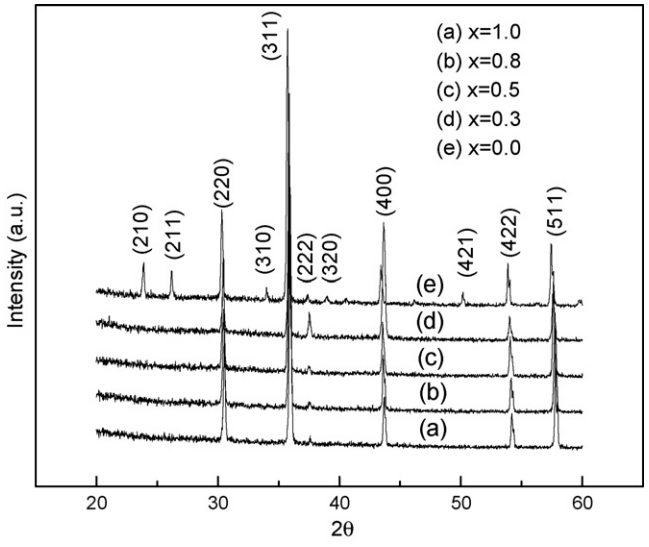

Fig. 1. XRD pattern of the sintered $Li_{0.5}Fe_{2.5-x}Cr_xO_4$ ferrites.

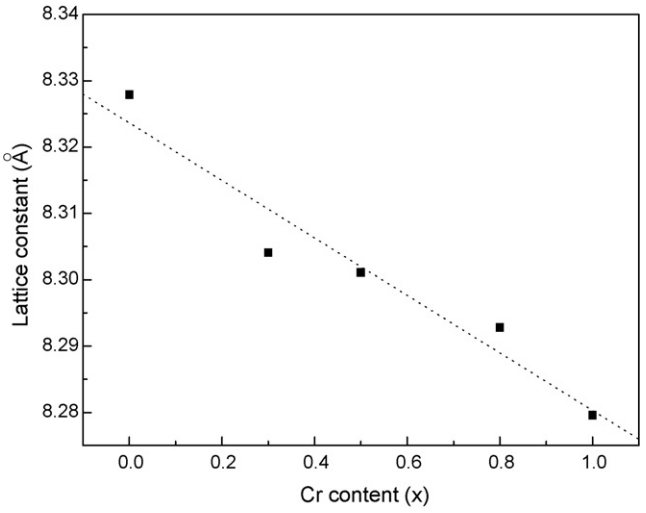

Fig. 2. Dependence of lattice constant on dopant concentration of Cr.

Table 1
Lattice constant, theoretical density, and cell volume of the $Li_{0.5}Fe_{2.5-x}Cr_xO_4$ system

Materials	Lattice constant (Å)	Theory density (g/cm^3)	Cell volume (Å^3)
$x = 0.0$	8.328	4.763	577.58
$x = 0.3$	8.304	4.773	572.63
$x = 0.5$	8.301	4.764	572.01
$x = 0.8$	8.293	4.752	570.31
$x = 1.0$	8.279	4.756	567.58

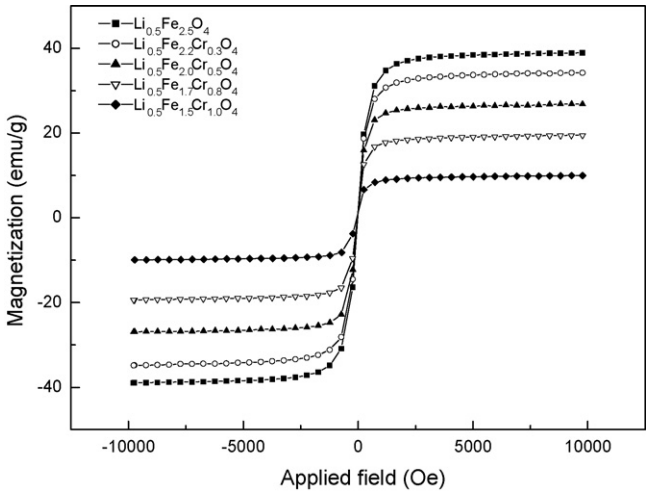

Fig. 3. Magnetization against applied field for $Li_{0.5}Fe_{2.5-x}Cr_xO_4$ powders.

Table 2
Magnetic properties of $Li_{0.5}Fe_{2.5-x}Cr_xO_4$ powder, an applied magnetic field of 10 kOe measured at room temperature

Materials	Saturation magnetization (emu/g)	Coercive force (Oe)	Remanent magnetization (emu/g)
$x = 0.0$	38.9	10.6	1.21
$x = 0.3$	34.8	21.7	1.72
$x = 0.5$	26.9	17.7	1.25
$x = 0.8$	19.4	19.3	1.27
$x = 1.0$	9.9	49.5	1.17

4.77–4.75 g/cm^3 for $Li_{0.5}Fe_{2.5-x}Cr_xO_4$ ($x = 0$–1.0). The lattice constant, theoretical density, and cell volume of the $Li_{0.5}Fe_{2.5-x}Cr_xO_4$ system sintered at 1200 °C for 4 h are summarized in Table 1.

The magnetization measurements for the $Li_{0.5}Fe_{2.5-x}Cr_xO_4$ specimens were carried out using a vibrating-sample magnetometer (VSM) at room temperature with an applied magnetic field of 10 kOe to reach saturation values. Introduction of Cr^{3+} ions into lithium ferrite greatly affects the magnetic properties. Fig. 3 plots the individually hysteresis loops for $Li_{0.5}Fe_{2.5-x}Cr_xO_4$ specimens. This figure indicates that the lithium ferrite is a soft magnetic material, which revealed minimal hystersis. The main magnetic properties of $Li_{0.5}Fe_{2.5-x}Cr_xO_4$ powders are listed in Table 2. Fig. 4 plots the saturation magnetization as a function of chromium content for $Li_{0.5}Fe_{2.5-x}Cr_xO_4$ specimens. Evidently, the saturation magnetization decreases linearly with increasing chromium content. This behavior is ascribed to the reason that as increasing with the concentration of non-magnetic ions weakens the inter-site exchange interaction, and the value of saturation magnetization decreases. $Li_{0.5}Fe_{2.5}O_4$ prepared by solid-state reaction and followed by annealed at 700 °C for 4 h exhibits an optimum magnetic property, saturation magnetization of 38.9 emu/g, remanent magnetization of 1.2 emu/g, and intrinsic coercive force of 10.6 Oe. It is well known that permeability of ferrite is strongly affected by saturation

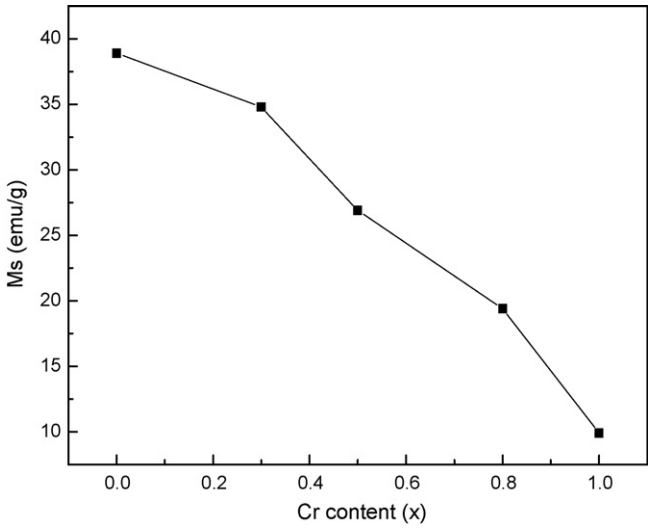

Fig. 4. The saturation magnetization as a function of chromium content for $Li_{0.5}Fe_{2.5-x}Cr_xO_4$ powders.

magnetization, crystal magnetization anisotropy, magnetostriction constant and internal stress. The equation of initial permeability is expressed as follows:

$$\mu_i = \frac{M_s^2}{aK + b\lambda\sigma}$$

where μ_i is initial permeability, M_s is saturation magnetization, K is crystal magnetic anisotropy, λ is magnetostriction constant, σ is internal stress, and a, b are constants [12]. If it is assumed that crystal magnetic anisotropy, magnetostriction, and internal stress are constant, the saturation magnetization is predominant in this equation. Since the $Li_{0.5}Fe_{2.5}O_4$ ferrite powder annealed at 700 °C possessed the highest saturation magnetization, the sintered $Li_{0.5}Fe_{2.5}O_4$ ferrite has the highest initial permeability among all specimens. Fig. 5 shows plot of the frequency dependence of initial permeability for sintered $Li_{0.5}Fe_{2.5-x}Cr_xO_4$ ferrite. It is observed that the initial permeability values of all specimens show the flat profile from 0.1 to 10 MHz and then rises to a maximum before falling rapidly

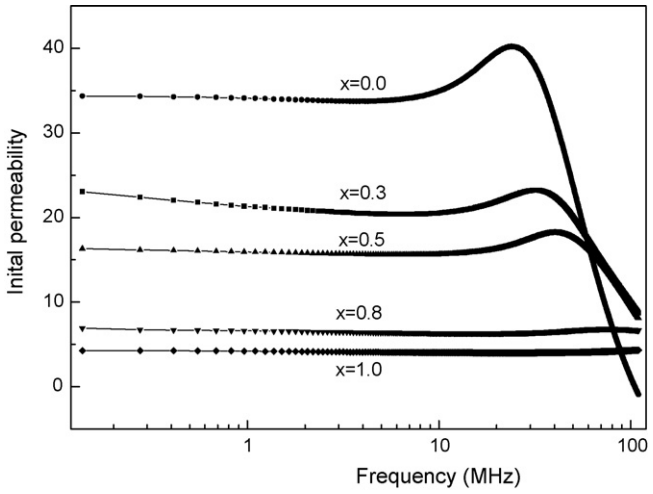

Fig. 5. Initial permeability of the sintered $Li_{0.5}Fe_{2.5-x}Cr_xO_4$ ferrites.

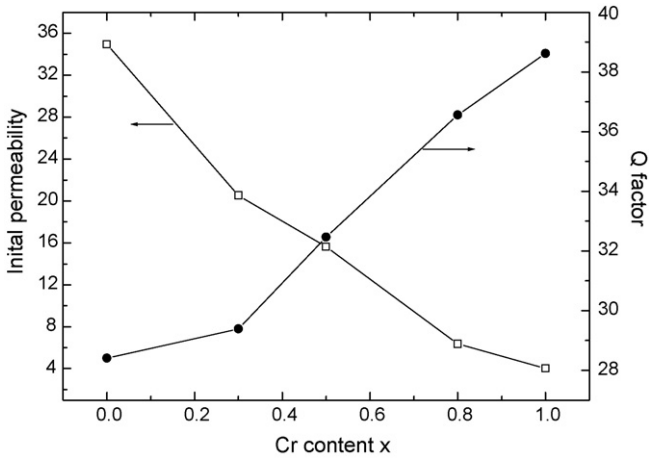

Fig. 6. Initial permeability and Q factor of the sintered $Li_{0.5}Fe_{2.5-x}Cr_xO_4$ ferrites at 10 MHz.

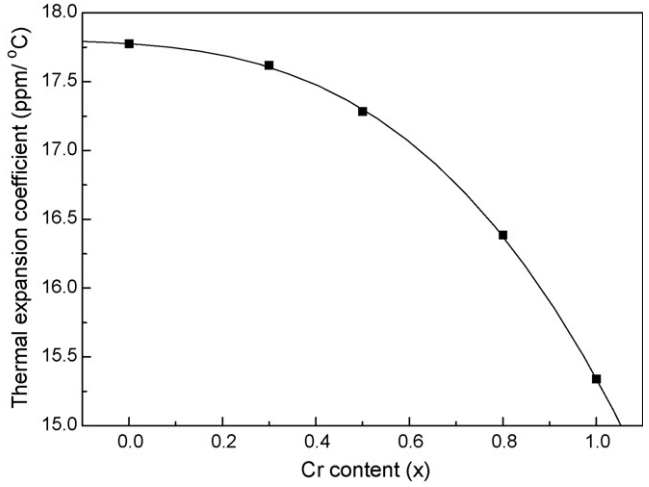

Fig. 7. Composition dependence of the average thermal expansion coefficient (30–850 °C) of the sintered $Li_{0.5}Fe_{2.5-x}Cr_xO_4$ ferrite.

to low values due to ferromagnetic resonance. The dispersion of initial permeability at low frequency is attributed to domain wall displacement. As increasing with Cr content for sintered $Li_{0.5}Fe_{2.5-x}Cr_xO_4$ ferrite, the resonance region shifts to a higher frequency. For use in magnetic applications, the initial permeability should remain fairly constant over certain frequency ranges. For sintered $Li_{0.5}Fe_{2.5}O_4$ ferrite, the initial permeability of 34 shows a flat profile from 0.1 to 10 MHz. The maximum initial permeability of 40 was obtained at 24.6 MHz. Fig. 6 reveals the initial permeability and Q factor as function of Cr content in $Li_{0.5}Fe_{2.5-x}Cr_xO_4$ specimens at 10 MHz. Obviously, Q factor increased with the Cr content from 28.4 for sintered $Li_{0.5}Fe_{2.5}O_4$ ferrite to 36.8 for the composition with $x = 1.0$, the initial permeability reached the maximum value of 34.9 for sintered $Li_{0.5}Fe_{2.5}O_4$ ferrite. Further increasing Cr content, the initial permeability decreased gradually from 20.5 for $x = 0.3$–4.0 for the composition with $x = 1.0$, respectively. The initial permeability was strongly influenced by the Cr content. For $Li_{0.5}Fe_{2.5}O_4$ specimen the initial permeability is the maximum value. However, further increasing the substituted amount of Cr, the initial permeability decreased. This result indicates that $Li_{0.5}Fe_{2.5}O_4$ exhibits maximum saturation magnetization. This phenomenon is in accordance with above equation.

Fig. 7 shows the dependence of the average thermal expansion coefficient. It indicates that the average thermal expansion coefficient decreases with increasing Cr content for $Li_{0.5}Fe_{2.5-x}Cr_xO_4$ ferrite. The average thermal expansion coefficient (ppm/°C) in the range of 25–850 °C give the polynomial correlation as follows, TEC $(x) = 17.775 - 0.216x - 0.723x^2 - 1.493x^3$ for $Li_{0.5}Fe_{2.5-x}Cr_xO_4$ ($x = 0.0$–1.0). The average thermal expansion coefficient of $Li_{0.5}Fe_{2.5-x}Cr_xO_4$ ($x = 0.0$–1.0) varied from 15.34 to 17.77. The correlation obtained provides an empirical evaluation of the properties of $Li_{0.5}Fe_{2.5-x}Cr_xO_4$ ferrite.

4. Conclusions

The effect of Cr content on lattice parameter, theoretical density, cell volume, magnetic and electronic properties were studied. Experimental results revealed that the lattice constant and cell volume decrease with the increasing of Cr content in $Li_{0.5}Fe_{2.5}Cr_xO_4$ specimens. The magnetic and thermal expansion properties of $Li_{0.5}Fe_{2.5}Cr_xO_4$ specimens are strongly affected by Cr content. The saturation magnetization decreases linearly with increasing chromium content. This behavior is ascribed to the reason that the increasing concentration of non-magnetic ions weakens the inter-site exchange interaction, and the value of saturation magnetization decreases. The initial permeability and the average thermal expansion coefficient of Cr-substituted lithium ferrite also decreases with increasing Cr content.

Acknowledgement

The author would like to thank the National Science Council of Taiwan for financial support of this research under Contract No. NSC 96-2221-E-259-005.

References

[1] X. Qi, J. Zhou, Z. Yue, Z. Gui, L. Li, Permeability and microstructure of manganese modified lithium ferrite prepared by sol–gel auto-combustion method, Mater. Sci. Eng. B 99 (2003) 278–281.
[2] H.M. Widatallah, C. Johnson, F. Berry, M. Pekala, Synthesis, structural, and magnetic characterisation of magnesium-doped lithium ferrite of composition $Li_{0.5}Fe_{2.5}O_4$, Solid State Commun. 120 (2001) 171–175.
[3] G.M. Argentina, P.D. Baba, Microwave lithium ferrite: an overview, IEEE Trans. Microw. Theory Technol. 22 (1974) 652–658.
[4] J.S. Baijal, S. Phanjoubam, D. Kothari, C. Prakash, P. Kishan, Hyperfine interactions and magnetic studies of Li–Mg ferrites, Solid State Commun. 83 (1992) 679–682.
[5] Y.P. Fu, C.S. Hsu, $Li_{0.5}Fe_{2.5-x}Mn_xO_4$ ferrite sintered from microwave-induced combustion, Solid State Commun. 134 (2005) 201–206.
[6] Y.P. Fu, Microwave-induced combustion synthesis of $Li_{0.5}Fe_{2.5-x}Cr_xO_4$ powder and their characterization, Mater. Res. Bull. 41 (2006) 809–816.
[7] Z. Yue, J. Zhou, X. Wang, Z. Gui, L. Li, Preparation and magnetic properties of titanium-substituted LiZn ferrites via a sol–gel auto-combustion process, J. Eur. Ceram. Soc. 23 (2003) 189–193.

[8] Y.P. Fu, Characterization of $Li_{0.5}Fe_{2.5-x}Cr_xO_4$ ferrite sintered from microwave-induced combustion, Jpn. J. Appl. Phys. 46 (2007) 7314–7316.
[9] E.W. Gorter, Saturation magnetization and crystal chemistry of ferrimagnetic oxides. I. II. Theory of ferrimagnetism, Philips Res. Rep. 9 (1954) 295–320.
[10] M.V. Kuznetsov, Q.A. Pankhurst, I.P. Parkin, Self-propagating high-temperature synthesis of lithium–chromium ferrites $Li_{0.5}Fe_{2.5-x}Cr_xO_4$ ($0 \leqq x \leqq 2.0$), J. Phys. D 31 (1998) 2886–2893.
[11] L. Fernandez-Barquin, M.V. Kuznetsov, Y.G. Morozov, Q.A. Pankhurst, I.P. Parkin, Combustion synthesis of chromium-substituted lithium ferrites $Li_{0.5}Fe_{2.5-x}Cr_xO_4$ ($x \leqq 2.0$): Rietveld analysis and magnetic measurement, Int. J. Inorg. Mater. 1 (1999) 311–316.
[12] M. Fjimotou, K. Hoshi, M. Nakazawa, S. Sekiguchi, Cu multiply twinned particle precipitation in low-temperature fired Ni–Zn–Cu ferrite, Jpn. J. Appl. Phys. I 32 (1993) 5532–5536.